

Few-body dynamics in ultrashort laser pulses

This article has been downloaded from IOPscience. Please scroll down to see the full text article.

2007 J. Phys.: Conf. Ser. 88 012045

(<http://iopscience.iop.org/1742-6596/88/1/012045>)

[The Table of Contents](#) and [more related content](#) is available

Download details:

IP Address: 128.138.140.133

The article was downloaded on 22/10/2008 at 21:19

Please note that [terms and conditions apply](#).

Few-body dynamics in ultrashort laser pulses

A Becker¹, C Ruiz¹, S Baier¹ and L Plaja²

¹ Max-Planck-Institut für Physik komplexer Systeme, Nöthnitzer Str. 38, D-01187 Dresden, Germany

² Departamento de Física Aplicada, Universidad de Salamanca, Salamanca, E-37008 Spain

E-mail: abecker@pks.mpg.de

Abstract. We present a model for ab-initio calculations of the interaction of two-electron atoms and molecules with few-cycle pulses of intense linearly polarised Ti:sapphire laser radiation. In the model the center-of-mass motion of the two electrons is restricted along the polarisation direction axis, while its relative coordinate and, hence, the electron correlation is retained in its full dimensionality. Results of numerical simulations exhibit the two pathways to nonsequential double ionization, namely the emission of a highly correlated electron pair upon rescattering and a delayed electron emission from a previously excited ion. Comparisons with the results of the usual one-dimensional approximation, in which the direction of each electron is restricted to the polarisation axis, are given. Distributions of the center-of-mass momentum and the correlated electron momenta along the polarisation direction are in qualitative agreement with the experimental data.

1. Introduction

Due to the development of high power Ti:sapphire laser systems light intensities of the order of 10^{20} W cm⁻² or above can be generated in the laboratories. The field strength at these intensities is a hundred times the Coulomb field binding the ground state electron in the hydrogen atom. As the laser intensities increased over the years the pulse lengths decreased to the femtosecond and the sub-femtosecond regime. The nonlinear interaction of atoms and molecules with such ultrashort and intense laser pulses has revealed a variety of interesting effects, namely above-threshold-ionization, high harmonic generation, laser induced tunneling, Coulomb explosion, multiple ionization and others. Atomic single ionization and other single-active-electron processes have been intensively studied for many years and the dynamical aspects in intense laser pulses are considered to be well understood nowadays. Within the single-active-electron approximation the outermost electron is assumed to be affected by the laser field only, neglecting the dynamic Coulomb correlation between the electrons in the atom. In the absence of electron correlation one would expect that multiple ionization proceeds via a sequential mechanism, in which the electrons are emitted one after the other by subsequent independent interaction with the external field. But, in experiments with linearly polarised near-infrared laser pulses (e.g. [1, 2, 3]) the hypothesis of a sequential multiple ionization mechanism has been disproved. In the low intensity range the observed double and multiple ionization yields exceed the expectations based on the sequential mechanism by many orders of magnitudes. The observations therefore provide the evidence of an effective nonsequential mechanism mediated via electron correlation.

It is nowadays widely accepted that the underlying mechanism for nonsequential ionization in a strong laser pulse is based on the following three-step or recollision process ([4, 5, 6], for recent reviews see e.g. [7, 8]): An electron, excited due to the interaction with the intense laser field in the continuum, is accelerated by the field, gains energy and can be driven back to the parent ion when the field changes its sign. Upon recollision it exchanges energy with the second electron via electron correlation interaction and either both electrons instantaneously leave the atom together or only one is detached leaving the second in an excited state, which is subsequently ionised by the field [9, 10, 11]. We may note that the rescattering mechanism can be seen as a strong-field extension of the two-step-one mechanism (TS1), known for single photon double ionization at low photon energies [12]. In the latter mechanism one electron absorbs the photon and knocks out the second electron on its way through the atom. Thus, while in the weak-field TS1 mechanism the electron correlation appears to be dominant on a very short time scale of a few attoseconds, in the strong-field rescattering mechanism there is a delay of about 2/3 of the laser period (about two femtoseconds at Ti:sapphire laser frequencies) between the interaction of the first electron with the field and the rescattering event.

Despite the success of the rescattering picture, further insights in the process would be provided by ab-initio calculation of the full laser driven two-electron dynamics. Simulations of the corresponding Schrödinger equation require the solution of a differential equation with six dimensions in space and one in time. Such computations at intensities of mid of 10^{14} W cm⁻² and near-infrared frequencies are, however, still at the limit of current high-power supercomputers [13, 14]. Under these circumstances, alternatives are systematic approximation methods, such as the intense-field many-body *S*-matrix theory (IMST), or a dimensional reduction of the many-body problem. The IMST is a thorough rearrangement of the usual many-body *S*-matrix series (for a review, see [7]) such that the dominant features of the process of interest appear in the first leading terms of the series. In the case of strong-field double ionization analysis of the terms up to second order has confirmed the rescattering mechanism as being the dominant process for nonsequential double ionization [15] and provided an interpretation of momentum and energy distributions of the emitted electrons (e.g. [10, 16, 17, 18]).

On the other hand, solutions of the time-dependent Schrödinger equation of model systems in reduced dimensions are known to reveal useful understanding of the temporal dynamics. Fundamental aspects of the single-active-electron dynamics in linearly polarised strong fields, e.g. in above-threshold-ionization or high harmonic generation, are retained in an one-dimensional approach, in which the electron motion is restricted to the direction of the field polarisation axis [19, 20]. Stimulated by this successful application, the one-dimensional approximation has been extended to the two-electron [21] and the three-electron problem [22] in the past. There occurs however a significant weak point in the one-dimensional approximation if applied to two or more electron systems. As outlined above, in nonsequential ionization besides the interaction with the strong external field the electron-electron interaction plays a dominant role. The latter does not show the same preferred directionality as the electron-field interaction. Consequently the one-dimensional model can generate results which are not in agreement with the experimental observations of nonsequential double ionization.

Below, we review an alternative two-electron approach [23], which goes beyond the conventional one-dimensional approximation. In that approach we have taken advantage of the fact that the external field couples to the center-of-mass of a two-electron (many-body) system, but not to its relative coordinate. Therefore, we have restricted the center-of-mass motion along the direction of a linearly polarised field, while the relative electron motion, which couples to the electron correlation interaction, is kept unchanged. The details of the dimensional reduction are discussed in the next section. The rest of the paper is organised as follows: We apply the model to the helium atom interacting with a few-cycle laser pulse. Analysis of snapshots of the electron distributions at different time instants during the pulse reveals different pathways to

nonsequential double ionization. The two-electron dynamics in the fully correlated model will be compared with results from the conventional one-dimensional approximation. We then present numerical results of the distributions of the center-of-mass momentum and the components of the correlated electron momenta along the polarisation axis. We end by summarising the results.

2. Two-electron model beyond the one-dimensional approximation

The two-electron Hamiltonian for a helium atom interacting with an electromagnetic pulse can be written in dipole approximation as (Hartree atomic units, $\hbar = m = e = 1$ are used):

$$H(\mathbf{R}, \mathbf{r}, t) = \frac{\mathbf{P}^2}{4} + \mathbf{p}^2 - \frac{\mathbf{P} \cdot \mathbf{A}(t)}{c} + \frac{1}{r} - \frac{2}{|\mathbf{R} + \frac{\mathbf{r}}{2}|} - \frac{2}{|\mathbf{R} - \frac{\mathbf{r}}{2}|} \quad (1)$$

where $\mathbf{R} = (\mathbf{r}_1 + \mathbf{r}_2)/2$, $\mathbf{P} = \mathbf{p}_1 + \mathbf{p}_2$, $\mathbf{r} = \mathbf{r}_1 - \mathbf{r}_2$, and $\mathbf{p} = (\mathbf{p}_1 - \mathbf{p}_2)/2$ are the center-of-mass and relative coordinates and associated momenta, respectively, and $\mathbf{A}(t)$ is the vector potential of the field. Please note that in the above form the two essential interactions for nonsequential double ionization, namely the electron-field interaction and the electron correlation, are decoupled in the two coordinates. Thus, one can take advantage of any directionality induced by the field by reducing the dimensions of the center-of-mass motion without changing the electron-electron interaction term. In case of linear polarisation it is reasonable to restrict the center-of-mass motion to the field direction ($\mathbf{P} \rightarrow P_Z$, $\mathbf{R} \rightarrow Z$), which results in a model Hamiltonian with only three degrees of freedom:

$$H(Z, \rho, z, t) = \frac{P_Z^2}{4} + p_\rho^2 + p_z^2 - \frac{P_Z A(t)}{c} + \frac{1}{\sqrt{\frac{\rho^2}{4} + z^2}} - \frac{2}{\sqrt{\frac{\rho^2}{4} + (Z + \frac{z}{2})^2 + a^2}} - \frac{2}{\sqrt{\frac{\rho^2}{4} + (Z - \frac{z}{2})^2 + a^2}}, \quad (2)$$

where z and ρ represent the relative coordinates of the two electrons parallel and perpendicular to the polarisation axis, respectively. Note that for a linearly polarised field the total angular momentum along the polarisation direction remains unchanged and hence, the Hamiltonian is symmetric in the relative coordinate over rotation about the polarisation axis. The parameter a^2 is introduced to soften the attractive Coulomb potentials in the numerical calculations.

Note that the model above is in the spirit of the one-dimensional approach of the single-active-electron Hamiltonians [19, 20]. But, it is a more general extension of it to many-electron systems than the usual restriction of the motion of each electron independently. The conventional one-dimensional approximation in two-electron systems [21] is obtained from the model Hamiltonian in Eq. (2) by diminishing the ρ -coordinate (and transforming it to the coordinate system of the individual electrons). Thus, it is the transversal direction of the relative coordinate and hence, the full consideration of the electron correlation interaction term, which puts the present model beyond the one-dimensional approach. Due to the restriction of the center-of-mass motion along the polarisation direction, the coordinates and momenta of the two electron perpendicular to the axis however have to be symmetric which introduces a correlation between the electrons that is not present in the unrestricted two-electron Hamiltonian in Eq. (1).

3. Application to helium atom: Results of numerical computations

Using the two-electron model we have performed ab-initio computations for helium atom [23] and hydrogen molecule with the two nuclei fixed along the polarisation axis [24, 25]. Below we will illustrate the results for the helium atom in comparison with those obtained from the conventional one-dimensional approximation (for the latter calculation we have set $\rho = 0$ in the Hamiltonian in Eq. (2)).

The calculations have been performed by propagating the wave function $\Psi(Z, \rho, z, t)$ using the Crank-Nicholson method on a grid. We have used a grid spacing of $\Delta\rho = \Delta z = \Delta Z = 0.3$

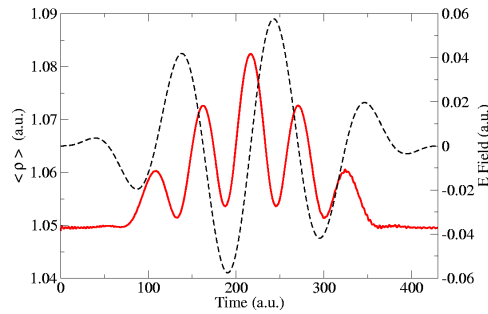


Figure 1. (Colour online) Expectation value $\langle \rho \rangle$ (red solid line) and electric field (black dashed line) as a function of time at a laser frequency $\omega = 0.057$ a.u. and a peak intensity $I_0 = 5 \times 10^{14}$ W/cm².

a.u. and 300 points in ρ -direction, 2000 points in z - and 2000 points in Z -direction; the time step was $\Delta t = 0.05$ a.u. The grid was chosen large enough to retain all essential parts of the double ionised part of the wave function on the grid for a momentum analysis at the end of the pulse. For the actual computation we have chosen a four-cycle laser pulse with a pulse envelope of $f(t) = \sin^2(\omega t/8)$. The carrier frequency of $\omega = 0.057$ a.u. corresponds to the Ti:sapphire laser wavelength of 800 nm, the peak intensity was 5×10^{14} W/cm². The initial ground state wavefunction of He has been obtained by imaginary time propagation. With $a^2 = 0.135$ the ground state energies of the neutral helium and the helium ion are -2.936 a.u. and -1.985 a.u., respectively. For the sake of comparison we have also performed one-dimensional calculations by setting $\rho = 0$ in Eq. (2); the grid and pulse parameters were analogous, but the smoothing parameter has been set to $a^2 = 0.32$ to get similar ground state energies of -2.9043 a.u. and -2.0057 a.u. for the helium atom and its ion.

A first impression of the relevance of the transversal direction of the relative coordinate in the fully correlated model is provided via its expectation value $\langle \rho \rangle$ (red solid line) as a function of time during the pulse, as shown in Fig. 1 (c.f. [23]). The temporal evolution of $\langle \rho \rangle$ is in full correspondence with the rescattering model: Whenever the electric field is zero, i.e. rescattering occurs, there is a maximum in the oscillation, indicating a strong electron correlation. While at the moments of (uncorrelated) single ionization, when the field is at its maxima, the expectation value is at minimum.

3.1. Pathways to nonsequential double ionization

Analysis of the evolution of the probability distribution of He atom [23] and H₂ molecule [24, 25] during one laser period have revealed the presence of two different pathways to nonsequential double ionization. The two mechanisms can be identified from the snapshots in Figs. 2 (at $t = 288$ a.u.) and 3 (at $t = 316$ a.u.). Shown are comparisons of (a) the (Z, z) -distribution obtained in the one-dimensional approximation, (b) the (Z, z) -distribution, integrated over ρ , and (c) the complementary view of the (ρ, z) -distribution, integrated over Z , both obtained using the fully correlated model. Please note that the diagonals in the (Z, z) -distributions represent the z_1 and z_2 axes, corresponding to single ionization; while between these axes the double ionization population is found.

In the snapshots shown in Fig. 2, taken close to a zero of the field, one sees in the (Z, z) -distribution of the fully correlated calculation (panel (b)) predominantly a correlated emission of two electrons at the same side of the core (in the $-Z$ direction). This contribution corresponds to a direct nonsequential double ionization upon rescattering via a binary electron-electron scattering [23, 26]. Since the two electrons leave the atom to the same side they exhibit

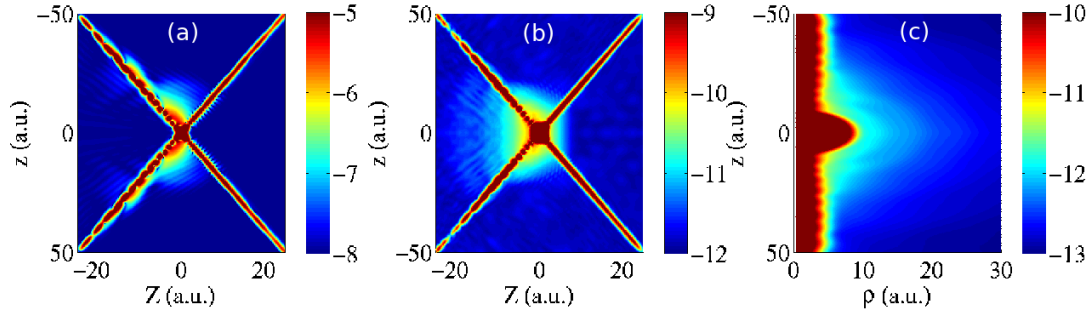


Figure 2. (Colour online) Comparison of the spatial probability distributions at $t = 288$ a.u.: (a) one-dimensional approximation, (b) fully correlated model integrated over ρ and (c) fully correlated model integrated over Z .

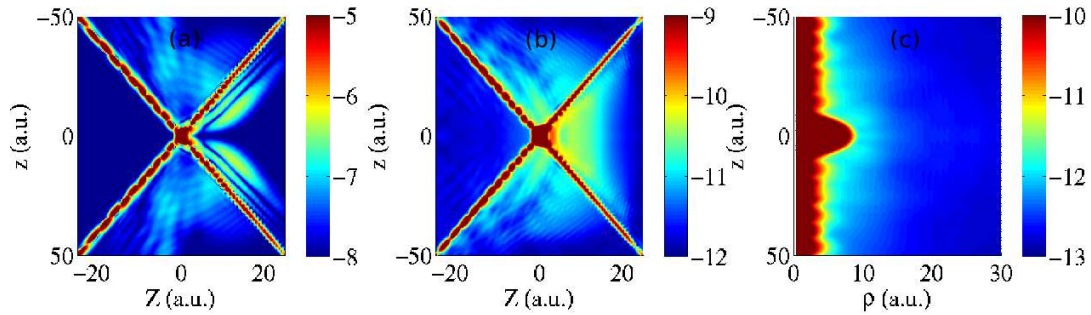


Figure 3. (Colour online) Same as Fig. 2 but at $t = 316$ a.u.

a strong transversal dynamics due to the Coulomb repulsion between them as it becomes apparent from the (ρ, z) -distribution in Fig. 2(c). We may note parenthetically that the smaller contributions of the double ionization population in the upper and lower triangles can be interpreted to correspond to a recoil collision, in which the returning electron is additionally backscattered at the nucleus after the primary electron-electron scattering [26]. The one-dimensional approximation does not take account of the transversal dynamics of the two correlated electrons. Consequently, the emission of the electron pair to the same side of the atom is strongly suppressed (c.f. Fig. 2(a)).

We now turn to the second set of snapshots taken shortly after the next field maximum and displayed in Fig. 3. One observes that the strongly correlated two-electron wavepacket emitted at the previous zero crossing of the field is now driven by the field towards the right triangle in the (Z, z) -distribution (panel b) and due to the long range Coulomb repulsion to larger ρ (c.f. (ρ, z) -distribution in panel (c)). But, there is a second new wavepacket released parallel to the z_1 and z_2 axes (upper and lower triangle of the double ionization region in Fig. 3(b)). This contribution is shown [23, 24, 25] to correspond to a field ionization of the singly ionised He^+ ion, predominantly from the excited states of the ion (c.f. [24]). In this pathway the second electron is released to the opposite direction of that of the first electron. Accordingly, the two electrons do not show a strong transversal dynamics in the ρ -direction (c.f. Fig. 3(c)). In the snapshot obtained using the one-dimensional approximation (Fig. 3(a)) this second pathway can be hardly identified. This is due to the fact that the contributions from the two pathways strongly interfere in the one-dimensional approximation, since they are not separated in the transversal direction as in the fully correlated model.

Before proceeding we note that it has been shown [24, 25] that both double ionization

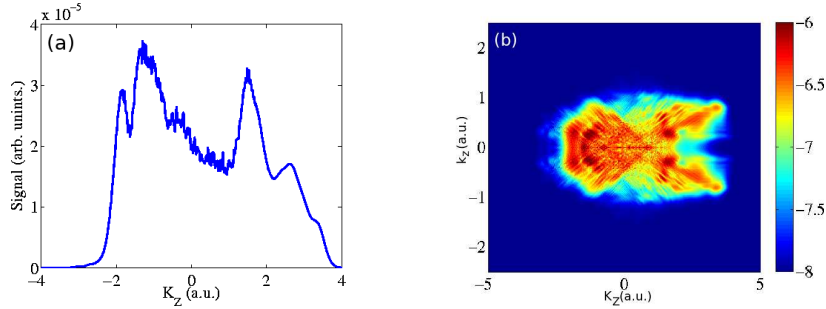


Figure 4. (Colour online) Final distribution of (a) the center-of-mass momentum and (b) the correlated electron momenta along the polarisation direction in the double ionization region as obtained from the fully correlated electron model. Horizontal axis: center-of-mass momentum K_Z , vertical axis: relative momentum component k_z .

mechanisms, identified above, are linked to the return of the initially singly ionised electron. This can be done by the use of absorbing boundaries in order to inhibit the return of some part of the singly ionised wave packet to the ion. As a result the double ionization population gets altered and eventually disappear completely, which is a clear evidence that rescattering is present in both mechanisms. Subtle patterns in the double ionization probability distributions have been identified to arise due to an interference of the contributions corresponding to the short and long quantum paths of the singly ionised electron wave packet.

3.2. Momentum distributions

Finally, we present in Fig. 4 the distributions of (a) the center-of-mass momentum and (b) the correlated electron momenta along the polarisation direction in the fully correlated electron model. The distributions are obtained at the end of the pulse from the double ionization population. To this end, we have partitioned the coordinate space as:

$$r_1 < 12 \text{ a.u. and } r_2 < 12 \text{ a.u.} : \text{ He atom} \quad (3)$$

$$r_1 < 6 \text{ a.u. and } r_2 \geq 12 \text{ a.u. or } r_1 \geq 12 \text{ a.u. and } r_2 < 6 \text{ a.u.} : \text{ He}^+ \text{ ion} \quad (4)$$

$$\text{complementary space} : \text{ He}^{2+} \text{ ion} \quad (5)$$

with $r_1 = \sqrt{(Z + \frac{z}{2})^2 + \frac{\rho^2}{4}}$ and $r_2 = \sqrt{(Z - \frac{z}{2})^2 + \frac{\rho^2}{4}}$.

The center-of-mass momentum distribution (Fig. 4(a)) is related the recoil ion momentum distributions obtained in the experiments [27, 28]. They show the characteristic double hump structure with a central minimum known for an ultrashort pulse (c.f. [23]). The side maxima and the asymmetry of the distribution arise because of the few-cycle pulse used in the present simulation. The correlated electron momenta distribution shows two prominent features: First, a maximum appears at $k_z = k_{a,z} - k_{b,z} = 0$ corresponding to an emission of an electron pair with the same momentum components along the polarisation direction, which is in agreement with the first experimental observations [29]. Furthermore, we observe a finger-like structure corresponding to an asymmetric energy sharing along the polarisation direction (c.f. [26]). Similar structures have been predicted in calculations at 400 nm wavelength using the unrestricted full two-electron Hamiltonian in Eq. (1) [14] and are observed in a recent high resolution, high statistic experiment [26]. The maximum for $k_z = 0$ can be attributed as due to a binary collision between the electrons, while the finger-like structure occurs due to a so-called recoil collision in which the returning electron is reflected by the nucleus after the collision with the electron [26].

4. Summary

In summary, we have presented ab-initio model calculations of the correlated two-electron dynamics in Helium atom interacting with an intense ultrashort few-cycle laser pulse. The model goes beyond the usual one-dimensional approximation, since it includes the electron correlation via the relative coordinate of the two electrons in its full dimensionality, while the center-of-mass motion is restricted to 1D along the polarisation axis. Application of the model to the Helium atom has been discussed and results of numerical calculations have been presented in comparison with those of the one-dimensional approximation. Two pathways to nonsequential double ionization are identified and characterised: First, the emission of a highly correlated electron pair near the zeros of the field showing a strong transversal dynamics. And, second, the electron emission from previously excited ionic states near the maxima of the field. Both mechanisms are found (c.f. [24, 25]) to be linked to the return of the single ionised electron wave packet to the ion. Results for the center-of-mass momentum distribution show a characteristic two hump structure, while those for the correlated electron momenta along the polarisation direction exhibit two features. Besides a maximum for an emission of both electrons with the same momentum components, a finger-like structure corresponding to an asymmetric energy sharing is found, in agreement with other numerical simulations and a high resolution experiment.

Acknowledgments

We acknowledge the contributions by F. He, P. Panek and A. Requate to the virtual laser lab NPSFLIB at the Max Planck Institute for the Physics of Complex Systems which has been used for the present calculations. We thank L. Roso for stimulating discussions. This work has been supported via DAAD (project no. D/05/25690), MEG (HA2005-0158), GGI-MEC (FIS2005-01351) and NSERC Canada (SRO grant no. 5796-299409/03).

References

- [1] L'Huillier A, Lompre L A, Mainfray G and Manus C 1982 *Phys. Rev. Lett.* **48** 1814
- [2] Walker B, Sheehy B, Di Mauro L F, Agostini P, Schafer K J and Kulander K C 1994 *Phys. Rev. Lett.* **73** 1227
- [3] Larochelle S, Talebpour A and Chin S L 1998 *J. Phys. B: At. Mol. Opt. Phys.* **31** 1215
- [4] Kuchiev M Yu 1987 *Sov. Phys.-JETP Lett.* **45** 404
- [5] Kuchiev M Yu 1995 *J. Phys. B: At. Mol. Opt. Phys.* **28** 5093
- [6] Corkum P B 1993 *Phys. Rev. Lett.* **71** 1994
- [7] Becker A and Faisal F H M 2005 *J. Phys. B: At. Mol. Opt. Phys.* **38** R1
- [8] Becker A, Dörner R and Moshhammer R 2005 *J. Phys. B: At. Mol. Opt. Phys.* **38** S753
- [9] LaGattuta K J and Cohen J S 1998 *J. Phys. B: At. Mol. Opt. Phys.* **31** 5281
- [10] Kopold R, Becker W, Rottke H and Sandner W 2000 *Phys. Rev. Lett.* **85** 3781
- [11] Feuerstein B, Moshhammer R, Fischer D, Dorn A, Schröter C D, Deipenwisch J, Lopez-Urrutia J, Höhr C, Neumayer P and Ullrich J 2001 *Phys. Rev. Lett.* **87** 043003
- [12] Samson J 1990 *Phys. Rev. Lett.* **65** 2863
- [13] Parker J S, Taylor K T, Clark C W and Blodgett-Ford S 1996 *J. Phys. B: At. Mol. Opt. Phys.* **29** L33
- [14] Parker J S, Doherty B J S, Taylor K T, Schultz K D, Blaga C I and DiMauro L F 2006 *Phys. Rev. Lett.* **96** 133001
- [15] Becker A and Faisal F H M 1996 *J. Phys. B: At. Mol. Opt. Phys.* **29** L197
- [16] Becker A and Faisal F H M 2000 *Phys. Rev. Lett.* **84** 3546
- [17] Becker A and Faisal F H M 2002 *Phys. Rev. Lett.* **89** 193003
- [18] Weckenbrock M, Becker A, Staudte A, Kammer S, Smolarski M, Bhardwaj V R, Rajner D M, Corkum P B and Dörner R 2003 *Phys. Rev. Lett.* **91** 123004
- [19] Javanainen J, Eberly J H and Su Q 1988 *Phys. Rev. A* **38** 3430
- [20] Su Q and Eberly J H 1991 *Phys. Rev. A* **44** 5997
- [21] Grobe R and Eberly J H 1992 *Phys. Rev. Lett.* **68** 2905
- [22] Ruiz C, Plaja L and Roso L 2005 *Phys. Rev. Lett.* **94** 063002
- [23] Ruiz C, Plaja L, Roso L and Becker A 2006 *Phys. Rev. Lett.* **96** 053001

- [24] Baier S, Ruiz C, Plaja L and Becker A 2006 *Phys. Rev. A* **74** 033405
- [25] Baier S, Ruiz C, Plaja L and Becker A 2007 *Laser Phys.* **17** 358
- [26] Staudte A, Ruiz C, Schöffler M, Schössler S, Zeidler D, Weber Th, Meckel M, Villeneuve D M, Corkum P B, Becker A and Dörner R *submitted for publication*
- [27] Weber Th, Weckenbrock M, Staudte A, Spielberger L, Jagutzki O, Mergel V, Urbasch G, Vollmer M, Giessen H and Dörner R 2000 *Phys. Rev. Lett.* **84** 443
- [28] Moshhammer R, Feuerstein B, Schmitt W, Dorn A, Schröter C, Ullrich J, Rottke H, Trump C, Wittmann M, Korn G and Sandner W 2000 *Phys. Rev. Lett.* **84** 447
- [29] Weber Th, Giessen H, Weckenbrock M, Staudte A, Spielberger L, Jagutzki O, Mergel V, Urbasch G, Vollmer M and Dörner R 2000 *Nature* **404** 608